Signal- and importin-dependent nuclear targeting of the kidney anion exchanger 1-binding protein kanadaptin

Stefan HÜBNER*[1], David A. JANS†, Chong-Yun XIAO†, Anna P. JOHN† and Detlev DRENCKHAHN*

*Institute for Anatomy and Cell Biology, Universität Würzburg, Koellikerstrasse 6, D-97070 Würzburg, Germany, and †Nuclear Signalling Laboratory, Division for Biochemistry and Molecular Biology, John Curtin School of Medical Research, Canberra, ACT 2601, Australia

Kanadaptin (kidney anion exchanger adaptor protein) has recently been identified as a protein with binding activity to the cytoplasmic domain of the kidney Na^+-independent Cl^-/HCO_3^- anion exchanger 1 (kAE1). Since it is widely expressed in tissues devoid of kAE1, however, kanadaptin is likely to have additional cellular roles. This is supported by its multidomain structure, and possession of three clusters of basic amino acids exhibiting similarity to known nuclear localization sequences (NLSs). In the present study, we use immunofluorescence and subcellular fractionation approaches to demonstrate that kanadaptin is localized within the nuclei of various epithelial and non-epithelial cultured cell types. The role of the different NLSs is examined in transfection studies using plasmids encoding full-length kanadaptin with or without green fluorescent protein (GFP) as a fusion tag, as well as truncation derivatives thereof. Strong nuclear localization of fusion proteins containing amino acids 140–230 of kanadaptin, which include the sequence AVSRKR-KA[193] (NLS1) was observed. Substitution of Arg[191] with a threonine residue resulted in a cytoplasmic location of the expressed protein, while NLS1 proved sufficient to target an otherwise cytoplasmically localized β-galactosidase–GFP fusion protein to the nucleus. Using a direct binding assay we show that a fusion protein containing kanadaptin amino acids 1–231 (but not the Thr[191] substituted derivative) is recognized with nM affinity by the conventional NLS-binding importin α/β heterodimer. Nuclear import studies on microinjected and permeabilized rat hepatoma cells demonstrated functionality of the NLS in nuclear targeting, with inhibition by antibodies demonstrating the requirement of both importin α and β for nuclear import of kanadaptin. That kanadaptin possesses a functional importin-α/β-recognized NLS explains the nuclear localization of kanadaptin in various cultured cell types, and opens up the possibility that kanadaptin may have a signalling role in the nucleus.

Key words: acid-secreting intercalated cells, nuclear import kinetics, nuclear localization sequence.

INTRODUCTION

Kanadaptin (kidney anion exchanger adaptor protein) has been recently identified in a yeast two-hybrid screen as a protein interacting with the cytoplasmic domain of the kidney Na^+-independent Cl^-/HCO_3^- anion exchanger 1 (kAE1) [1], which is an alternatively spliced isoform of the erythroid AE1 (band 3). kAE1 localizes to the basolateral membrane of acid-secreting intercalated cells (referred to as type A intercalated cells) in rabbit kidney collecting ducts [2]. Transcription of kAE1 in the kidney of rat [3,4], mouse [5] and human [6] occurs from an alternative transcription initiation site within intron 3, which results in the lack of the first 78 and 65 amino acids respectively in rodent and human. Together with the apical proton-secreting vacuolar type H^+-ATPase [7], kAE1 plays an essential role in the final urinary acidification in the connecting segment and the cortical and medullary collecting ducts.

Immunofluorescence studies in rabbit kidney described diffuse distribution of kanadaptin throughout the cytoplasm of all epithelial cells of the collecting duct [1]. In type A intercalated cells, kanadaptin was reported to co-localize with kAE1 in cytoplasmic vesicles, but not with kAE1 along the basolateral plasma membrane. This led to the suggestion that kanadaptin might play a role in the targeting of kAE1-containing vesicles to the basolateral cell surface. However, consistent with the immunostaining of kanadaptin, not only in type A intercalated cells but also in cells of the collecting duct not expressing kAE1, is the observation that kanadaptin transcripts are also expressed in tissues other than kidney, including lung, liver, brain, testis and heart [1], suggesting additional roles for kanadaptin.

We undertook detailed analysis of the mouse kanadaptin sequence, results indicating that kanadaptin is a multidomain protein (see Figure 1A). Of particular interest was the identification of sequences similar to nuclear localization sequences (NLSs), implying that kanadaptin may have an intracellular signalling role in communicating between the cytoplasmic and nuclear compartments. As a first step towards determining whether nuclear translocation could be a property of kanadaptin, its intracellular distribution was investigated in transfection studies using plasmids encoding kanadaptin–green fluorescent protein (GFP) and kanadaptin–β-galactosidase (β-Gal) fusion proteins. Bacterially expressed proteins were used for *in vivo* and *in vitro* nuclear import assays and for binding studies with proteins of the importin family known to mediate NLS-dependent nuclear import [8,9]. The results indicate that kanadaptin contains a functional NLS within its N-terminus that is recognized by importin-α/β and that this NLS is sufficient to target a large heterologous protein to the nucleus. This

Abbreviations used: CLSM, confocal laser scanning microscopy; DMEM, Dulbecco's modified Eagle's medium; DSRM, double-stranded RNA-binding motif; DTT, dithiothreitol; β-Gal, β-galactosidase; GFP, green fluorescent protein; GST, glutathione S-transferase; GTP[S], guanosine 5′-[γ-thio]triphosphate; HEK, human embryonic kidney; IPTG, isopropyl β-D-thiogalactoside; kAE1, kidney Na^+-independent Cl^-/HCO_3^- anion exchanger 1; MDCK, Madin–Darby canine kidney; L-M(TK−) fibroblasts, fibroblasts from a thymidine kinase-deficient mouse L cell line; MEM, minimum essential medium; NLS, nuclear localization sequence; bpNLS, bipartite NLS; NP-NLS, nucleoplasmin NLS; NPC, nuclear pore complex; SH3, Src homology 3; T-ag, simian virus 40 large tumour antigen.

[1] To whom correspondence should be addressed (e-mail stefan.huebner@mail.uni-wuerzburg.de).

opens up the possibility that kanadaptin may have a role in communicating signals to the nucleus, which is supported by our observation that kanadaptin is concentrated within the nucleoplasm of various cultured cells derived from epithelial and non-epithelial tissues.

MATERIALS AND METHODS

Construction of GFP-derived expression plasmids

The GFP expression plasmids used in the present study are shown in Figure 1(B). They were all derived from expression plasmids pEGFPC1 or pEGFPN3 (ClonTech Laboratories) except for plasmid β-Gal–NLS1–GFP, which was derived from plasmid pHM829 [10]. Expression plasmids pGFP–K1 and pK1–GFP were generated from the PCR-amplified mouse kanadaptin coding region using expression plasmid pGEX-2TK-kanadaptin [1] as a template and the primers: 5′-CCGCTCGAGCCATGCGCTTTGGAGGCAGC-3′ and 5′-GGAATTCCAGTAGCCATACTTGTCATTAAG-3′ (introduced restriction sites for *Xho*I and *Eco*RI are underlined). The PCR product was gel-purified and subcloned in frame with the cDNA encoding GFP using *Xho*I/*Eco*RI-digested plasmids pEGFPC1 and pEGFPN3 respectively, to yield pGFP–K1 and pK1–GFP. Plasmid pGFP–K2 was obtained by digesting pGFP–K1 sequentially with *Hin*dIII and *Sma*I. The *Hin*dIII site was filled-in and the deleted plasmid was gel-purified and re-ligated. Plasmid pGFP–K3 was created in analogous fashion by using *Bst*EII instead of *Hin*dIII. Plasmid pGFP–K4 was obtained by PCR amplification using pGFP–K1 as a template and the primers: 5′-CCGGGTACCAGGTTACCTGTAGATGATTC-3′ and 5′-CCGGGTACCAAGCTTCCCAGCCTTCTTCATC-C-3′ (introduced *Kpn*I site underlined), followed by digestion of the PCR product with *Kpn*I, gel-purification and subcloning into the *Kpn*I site of pEGFPC1. Plasmids pGFP–K5 and pK5–GFP were created in analogous fashion to pGFP–K2 by digesting pGFP–K1 and pK1–GFP sequentially with *Bst*EII and *Hin*dIII, restriction sites filled-in, and the deleted plasmid gel-purified and re-ligated. Plasmid pGFP–K6 was derived from pGFP–K1 using site-directed mutagenesis (Transformer™ Site-Directed Mutagenesis Kit; ClonTech Laboratories), and mutagenic primer 5′-AGTATCTCGGAAAACGAAAGCCAAGAAC-3′ [converting NLS1 (^{189}RKRK) into ΔNLS1 (^{189}RKTK)] and selection primer 5′-TGCATTAGTTCTTAAGAGTAATCAATTAC-3′ (converts a *Vsp*I site into an *Afl*II site in plasmid pEGFPC1). Plasmid pK1–ΔGFP was derived from plasmid pK1–GFP by deleting the cDNA encoding GFP using *Eco*RI and *Xba*I. Re-ligation of the gel-purified GFP-cDNA-deleted plasmid was performed after filling-in with Klenow polymerase.

In all cases, the integrity of constructs was confirmed by sequencing. Expression of GFP fusion proteins and kanadaptin was monitored by Western-blot analysis of extracts from transfected human embryonic kidney (HEK)-293 cells using a GFP-specific antibody (ClonTech Laboratories) or a mouse monoclonal antibody against kanadaptin (Transduction Laboratories).

The plasmid β-Gal–NLS1–GFP was derived from expression plasmid pHM829 [10] by inserting a double-stranded synthetic oligonucleotide cassette containing a *Xba*I-specific 5′ overhang (underlined): 5′-CTAGGGCAGTATCTCGGAAAAGGAAA-GCCC-3′ (NLS1 sense) and 5′-CTAGGGGCTTTCCTTTTCC-GAGATACTGCC-3′ (NLS1 antisense), encoding NLS1 (amino acids 187–193) of kanadaptin, between the β-Gal and GFP coding sequences using the *Xba*I site. Plasmids β-Gal–NP-NLS and β-Gal–GFP either containing or lacking the nucleoplasmin NLS (NP-NLS; ^{189}KRPAATKKAGQAKKKK) respectively, were similarly derived from plasmid pHM829 [10].

Construction of 6 × His-tagged expression plasmids

For construction of plasmid p6 × His–K1, the kanadaptin coding region was first subcloned as a *Sal*I/*Eco*RI-digested cDNA fragment into the corresponding sites of bacterial expression vector pRSETA (Invitrogen). The *Xho*I/*Eco*RI-digested cDNA fragment was obtained from pGEX2T-kanadaptin as described above [1]. The expression plasmids p6 × His–K1 and p6 × His–K1ΔNLS1 were then derived containing the N-terminal 231 amino acids of kanadaptin, with NLS1 mutated in 6 × His–N-ΔNLS1. Plasmid p6 × His–K1 was obtained by deleting the C-terminus of the kanadaptin coding region using an internal *Hin*dIII site and a pRSETA *Hin*dIII site at the 3′-terminus. The *Hin*dIII sites were converted into blunt ends and the gel-purified expression plasmid encoding C-terminal truncated kanadaptin re-ligated. Construction of p6 × His–K1ΔNLS1 was achieved by initially replacing an internal *Bst*EII/*Hin*dIII cDNA fragment with the fragment from pGFP–K6 carrying the mutated NLS1, followed by deletion of the 5′-terminus as per the construction of p6 × His–K1.

In order to study subcellular localization of full-length kanadaptin in cultured cells, expression vector pK1–6 × His was constructed using plasmid pK1–GFP. The GFP moiety was deleted by *Xba*I/*Eco*RI digestion (creating expression plasmid pK1–ΔGFP, see above), followed by treatment with Klenow polymerase, to generate blunt ends, and gel-purification. Following re-ligation the regenerated *Eco*RI site was used to insert a double-stranded synthetic oligonucleotide cassette encoding six histidine residues. As above, construct integrity was confirmed by DNA sequencing. Expression of K1–6 × His was monitored by Western-blot analysis of extracts from transfected HEK-293 cells using a mouse monoclonal 6 × His-specific antibody (Qiagen).

Cell culture and transfection

HEK-293, HeLa and Madin–Darby canine kidney (MDCK) cells, as well as fibroblasts from a thymidine kinase-deficient mouse L cell line [L-M(TK −) fibroblasts], were maintained in a humidified incubator at 37 °C under a 5% CO_2 atmosphere in minimum essential medium (MEM) or Dulbecco's modified Eagle's medium (DMEM) that was supplemented with 10% (v/v) fetal calf serum, 50 units/ml penicillin, 50 units/ml streptomycin and 2 mM L-glutamine. The human pluripotential teratocarcinoma cell line NT2/D1 was maintained in OptiMEM, supplemented with 5% (v/v) fetal calf serum, 50 units/ml penicillin, 50 units/ml streptomycin and 2 mM L-glutamine. One day prior to transfection, 2.5×10^5 cells were seeded on to gelatin-coated glass coverslips and allowed to grow for 24 h to subconfluency. HEK-293 and HeLa cells were then transiently transfected with 10–20 μg of vector DNA using the $CaPO_4$ method [11]. In the case of subconfluent MDCK cells, transient transfection was carried out in the presence of Effectene (Qiagen) and 2 μg of vector DNA. For generation of a stable cell line expressing GFP–K1, the transfected cells were incubated in medium supplemented with the antibiotic Geneticin (G418; Life Technologies). Individual clones were isolated by ring cloning. Cells of the HTC rat hepatoma tissue culture line (a derivative of Morris hepatoma 7288C) were cultured in DMEM, supplemented with 10% (v/v) fetal calf serum as previously described [12,13].

Fluorescence microscopy

Visualization of endogenous kanadaptin in cultured cells was performed using a mouse kanadaptin-specific monoclonal antibody (see above). Cells mounted on coverslips were fixed with

4% (w/v) formaldehyde in PBS for 10 min at 22 °C, then permeabilized with 0.25% Triton X-100 in PBS for 5 min and incubated with the primary antibody for 20 h at 4 °C. Cells were then incubated with a Cy3-conjugated goat anti-mouse antibody for 1 h at 22 °C and finally mounted with 60% (w/v) glycerol in PBS containing the anti-fade agent n-propyl gallate [1.5% (w/v)].

Visualization of the subcellular localization of GFP–kanadaptin fusion proteins in living cells was performed 24 h after transfection of HEK-293, HeLa or MDCK cells with GFP–kanadaptin fusion protein-expressing vector DNA. Cells mounted on coverslips were rinsed with PBS, mounted with 60% (w/v) glycerol in PBS containing 1.5% (w/v) n-propyl gallate and examined directly by confocal laser scanning microscopy (CLSM) using a Bio-Rad MRC 600 system equipped with an Olympus BH2-RFCA microscope and an Olympus 63 × Planapo objective. Images were converted into Photoshop format using Lasergene 2.1 software. Detection of untagged and 6 × His-tagged kanadaptin in MDCK cells was carried out by immunofluorescence using either the mouse kanadaptin antibody or a monoclonal mouse tetra-His antibody (Qiagen) as described above.

Cell fractionation

L-M(TK −) fibroblasts and human embryonic teratocarcinoma NT2/D1 cells grown to confluence were washed once with PBS, twice with 10 mM Hepes (pH 7.3), 110 mM potassium acetate, 2 mM magnesium acetate and 2 mM dithiothreitol (DTT), and then incubated for 10 min on ice in hypotonic buffer [5 mM Hepes (pH 7.3), 10 mM potassium acetate, 2 mM magnesium acetate, 2 mM DTT and 1 mM PMSF] to let the cells swell. Cells were then lysed by ten strokes through a 1.5 inch, 22 gauge needle. Nuclei of disrupted cells were subsequently collected by centrifugation at 2000 ***g*** for 10 min. The resulting supernatant was centrifuged again at 10000 ***g*** for 20 min (at 4 °C) to yield the cytosolic fraction. Both fractions were assayed for protein concentration using the Bradford protein assay [14]. BSA was used as a standard.

Expression and purification of His- and glutathione S-transferase (GST)-tagged fusion proteins

Isopropyl β-D-thiogalactoside (IPTG; 1 mM) in 100 ml of Luria–Bertani medium was used to induce expression of 6 × His–K1 and 6 × His–K1ΔNLS1 fusion proteins in *Escherichia coli* strain BL21 (DE3) pLysS for approx. 4 h at 37 °C. IPTG-induced *E. coli* cells were subsequently resuspended in 2 ml of buffer A [50 mM NaH_2PO_4 (pH 8.3), 300 mM NaCl, 1 mM imidazole and 1 mg/ml lysozyme] and disrupted by successive freeze–thaw cycles followed by sonication. Insoluble material was removed by centrifugation and the supernatant was loaded on to a Ni^{2+}-nitrilotriacetate column (Qiagen). After washing the column with buffer B [50 mM NaH_2PO_4 (pH 8.3), 300 mM NaCl and 20 mM imidazole], the fusion proteins were eluted with buffer C [50 mM NaH_2PO_4 (pH 8.3), 300 mM NaCl and 250 mM imidazole] and dialysed against intracellular buffer (110 mM KCl, 5 mM $NaHCO_3$, 5 mM $MgCl_2$, 1 mM EGTA, 0.1 mM $CaCl_2$, 20 mM Hepes, 1 mM DTT and 5 μg/ml leupeptin, pH 7.4). The amount of expressed fusion protein was determined by the method of Bradford [14]. Integrity and purity of expressed His-tagged fusion proteins were assayed by SDS/PAGE, followed by Coomassie Brilliant Blue staining. The expression and purification of mouse importin α and β GST fusion proteins were performed as described previously [15,16]. GST-free importin α was prepared by thrombin cleavage as described previously [15,16].

Importin binding

An ELISA-based binding assay [16–18] was used to examine the binding affinity between importin subunits and 6 × His–K1 and 6 × His–K1ΔNLS1. The latter were coated on to 96-well microtitre plates and incubated with increasing concentrations of importin subunits (importin α–GST, importin β–GST and, in the case of the NLS receptor heterodimer, precomplexed importin α and importin β–GST). Detection of bound importin–GST was performed using an anti-GST primary antibody, an alkaline phosphatase-coupled rabbit anti-goat secondary antibody and *p*-nitrophenyl phosphate as substrate. Absorbance measurements were performed over 90 min using a plate reader (Molecular Devices), with values corrected by subtracting absorbance both at 0 min and in wells incubated without importin subunits.

Nuclear import assays

The nuclear import kinetics of 6 × His–K1 and 6 × His–K1ΔNLS1, labelled with 5-iodoacetamido-fluorescein (IAF) as previously described [12], were determined in both microinjected (*in vivo*) [12,13] and mechanically perforated (*in vitro*) [12] HTC cells in conjunction with CLSM. In the case of microinjected cells, HTC cells were fused with poly(ethylene glycol) approx. 1 h prior to microinjection to produce polykaryons [12]. Quantification of fluorescence has been previously described in detail [19–22]. Nuclear accumulation was also examined *in vitro* in the presence of 1% (w/v) glycerol and 0.025% CHAPS, which results in permeabilization of the nuclear envelope. Accumulation of proteins under these conditions results solely from binding to nuclear components [17,23]. Inhibition experiments in the presence of antibodies specific to either importin α or importin β were performed as previously described [24]. The dependence on the guanine nucleotide-binding protein Ran was tested by pretreating cytosolic extract with guanosine 5′-[γ-thio]triphosphate (GTP[S]) [17,23].

RESULTS

Multidomain structure of kanadaptin

Detailed analysis of the kanadaptin sequence, performed using the PROSITE database [25,26] and by SMART (a simple modular architecture research tool) [27,28], indicated a multidomain structure (Figure 1A). This included a Src homology 3 (SH3) domain-binding sequence (^{365}LPPKRPELPP), which is a proline-rich sequence with the core sequence 'PXXP' (where X is any amino acid other than cysteine) [29], a glutamic acid-rich domain (E-motif) of unknown function, and a leucine zipper domain (^{244}LNDAERELAEISERLKASSKVL), which is a dimerization motif typical of transcription factors. In addition, an ATP/GTP-binding motif A (P-loop; ^{56}ANTTEGKS) and a double-stranded RNA-binding motif (DSRM; amino acids 108–177) could be identified near the N-terminus.

Of particular interest was the identification within the kanadaptin sequence of three putative NLSs, two of which [^{189}RKRK (NLS1) and ^{458}PKKKKSP (NLS2); see Figure 1] resemble the NLS of simian virus 40 large tumour antigen (T-ag; ^{126}PKKKRKV) [30–32]. The third NLS (^{325}KKTELQTTNAENKTKKL) resembles the bipartite NLS (bpNLS) of nucleoplasmin [33] and consists of two clusters of basic amino acid residues separated by a 10–12 amino acid spacer. Both T-ag-like NLSs and bpNLSs have been shown to be recognized by the 'NLS receptor', the importin α/β heterodimer [17,24,34–37]. The kanadaptin NLSs are surrounded by numerous potential phosphorylation sites for kinases, such as protein kinase CK2, cAMP-dependent protein kinase and protein kinase C, which is

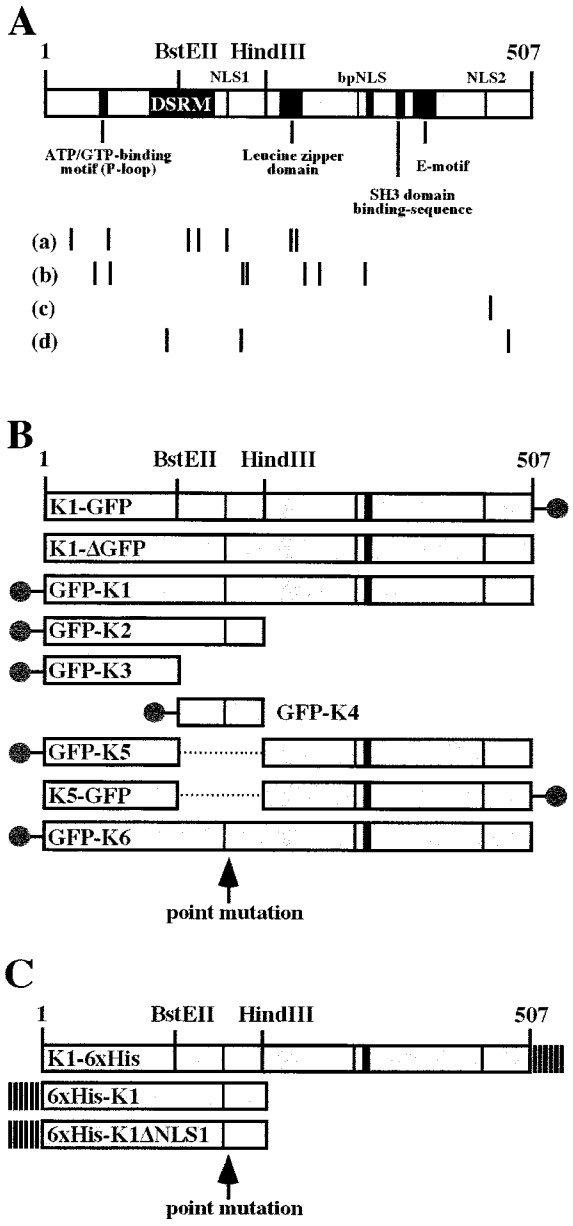

Figure 1 Sequence elements of kanadaptin (A) and expression constructs used in the present study (B and C)

The domain structure of kanadaptin was analysed using the PROSITE [25,26] and PSORT protein localization prediction [45] programs, and by SMART analysis [27,28]. Sequence elements (single-letter amino-acid code) indicated in (**A**) are: NLS1 (^{189}RKRK); bpNLS (^{325}KKTELQTTNAENKTKKL); NLS2 (^{458}PKKKKSP); DSRM (amino acids 108–177); ATP/GTP-binding motif A (P-loop; ^{56}ANTTEGKS); leucine zipper domain (^{244}LNDAERELAEISER-LKASSKVL); glutamic-acid rich domain (E-motif; ^{386}EEEEEEEEEEEEKEEHEE), and proline-rich SH3 domain-binding sequence (^{365}LPPKRPELPP). Putative sites for protein kinases are indicated: protein kinase C (a); protein kinase CK2 (b); cAMP-dependent protein kinase (c); and tyrosine kinase (d). (**B**) GFP fusion proteins used in the present study. The location of the NLSs and restriction sites chosen for expression plasmid construction are indicated. (**C**) The His-tagged fusion proteins used in the present study. ●, GFP; ||||||, 6 × His-tag.

of significance in view of the fact that phosphorylation close to or within NLSs is known to regulate NLS function and thereby NLS-dependent nuclear protein import [20,38]. The multidomain structure of kanadaptin, and in particular the presence of multiple NLSs, suggested that kanadaptin may play an important intracellular role through its ability to translocate from the cytoplasmic compartment into the nucleus, and thereby be part of a cytoplasmic–nuclear signalling pathway in analogous fashion to the plaque protein β-catenin [39].

Nuclear localization of kanadaptin in cultured cells

The subcellular localization of endogenous kanadaptin was analysed by immunofluorescence and CLSM in various cell lines, such as MDCK cells, HeLa cells, L-M(TK−) fibroblasts and human pluripotential teratocarcinoma NT2/D1 cells (Figure 2A). In all of the cell lines, nuclear immunostaining for kanadaptin could be detected. Nuclear staining was not due to cross-reactivity of the antibody with other nuclear proteins, since anti-kanadaptin antibody only reacted with a single protein of the size of kanadaptin (approx. 57 kDa) as shown by Western-blot analysis of cell extracts (Figure 2B). Specific staining for kanadaptin was also observed after Western-blot analysis in crude homogenates and in nuclei of human endothelial ECV304 cells, as well as human A-431 squamous carcinoma cells (results not shown). Cytosolic and nuclear fractions were prepared from L-M(TK−) fibroblasts and NT2/D1 cells, and equal amounts of proteins were loaded on to SDS gels for subsequent Western-blot analysis. We found kanadaptin solely in the nuclear fractions of L-M(TK−) fibroblasts and NT2/D1 cells (Figure 2C, lanes 3 and 6). An antibody specific for mouse histone H1.2 served as a nuclear marker (Figure 2D). Neither kanadaptin nor histone H1.2 were detected in the cytoplasmic fraction (Figures 2C and 2D, lanes 2 and 7). These results clearly demonstrate that endogenous kanadaptin is predominantly nuclear in a variety of cell types.

Identification of sequences required for nuclear translocation of kanadaptin

As a first step toward determining the subcellular distribution pattern of kanadaptin, a cDNA encoding full-length kanadaptin and cDNA fragments thereof were fused in frame to the coding sequence of GFP. The GFP fusion proteins used in the present study are depicted schematically in Figure 1(B). The subcellular localization of the GFP fusion proteins expressed in living cells was visualized using CLSM 24 h post-transfection and carried out in MDCK cells due to the fact that they possess endogenous kanadaptin, and hence are appropriate, physiologically relevant cells in which to assess subcellular localization of overexpressed protein. In addition, MDCK cells (derived from the dog distal nephron) express many characteristics of the renal collecting duct [40,41]. As shown in Figure 3(D), we found exclusively nuclear accumulation and nucleolar exclusion of transiently expressed GFP–K1 in MDCK cells. Wild-type GFP, serving as a control, displayed distribution throughout the cytoplasmic and nuclear compartments (Figure 3C), consistent with the size of GFP of 27 kDa which allows free diffusion into the nucleus through the nuclear pore complex (NPC). Nuclear accumulation was also observed after transient expression of GFP–K1 in HEK-293 and HeLa cells (Figures 3A and 3B), and when GFP was fused to the C-terminus of kanadaptin (K1–GFP; results not shown), indicating that nuclear accumulation of kanadaptin occurred irrespective of the position of the GFP moiety.

Subcellular localization was also examined in stably transfected MDCK cells. Exclusive nuclear fluorescence was observed in the case of GFP–K1 (Figure 3D'), in contrast with GFP alone which was found throughout the cell in both cytoplasm and nucleus in all three cell types studied (results not shown). To exclude the possibility of any contribution of the GFP moiety on nuclear accumulation of kanadaptin and to demonstrate full-length

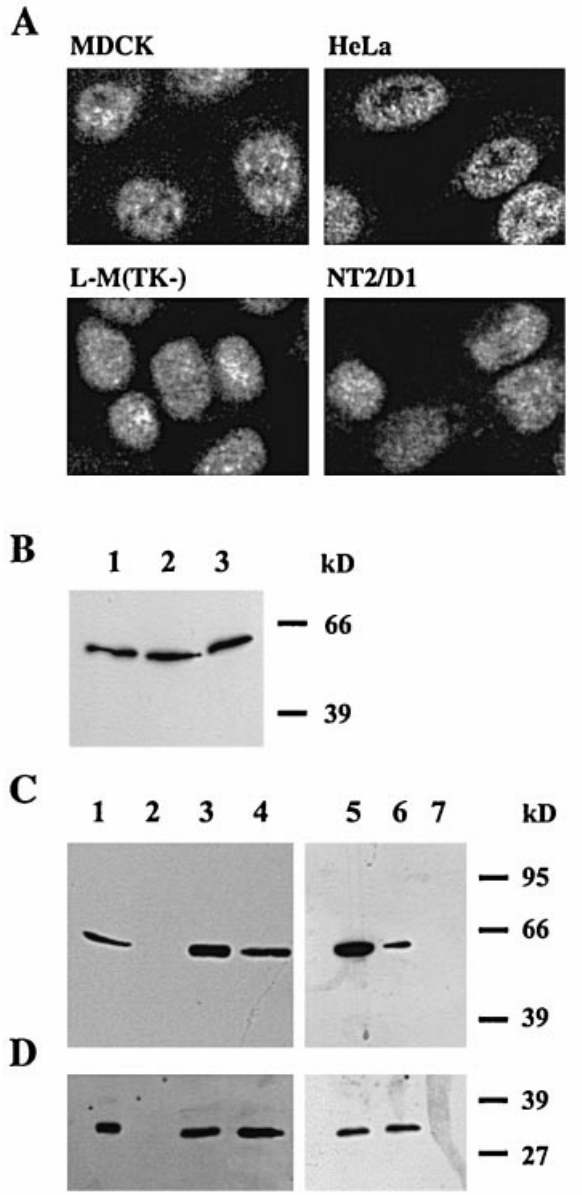

Figure 2 Subcellular distribution of kanadaptin

(**A**) Fluorescent visualization by CLSM of the subcellular localization of endogenous kanadaptin using an anti-kanadaptin antibody and immunofluorescence in MDCK cells, HeLa cells, L-M(TK−) fibroblasts and human teratocarcinoma NT2/D1 cells. No significant nuclear staining was observed in the presence of the secondary antibody alone (results not shown). (**B**) Western-blot analysis for kanadaptin in crude homogenates of MDCK (lane 2) and HeLa (lane 3) cells using anti-kanadaptin antibody. A rat kidney crude homogenate (lane 1) served as a positive control. (**C** and **D**) Western-blot analysis for kanadaptin using the anti-kanadaptin antibody (**C**), or for histone H1.2 using an anti-(histone H1.2) specific antibody (**D**), in rat kidney crude homogenate (lane 1) and subcellular fractions of L-M(TK−) fibroblasts (lane 2, cytosol; lane 3, nuclear; lane 4, crude homogenate) and human teratocarcinoma NT2/D1 cells (lane 5, crude homogenate; lane 6, nuclear; lane 7, cytosol). Crude homogenates were prepared by lysis of cells in Laemmli sample buffer. The rat kidney crude homogenate was obtained from Transduction Laboratories. kD, kDa,

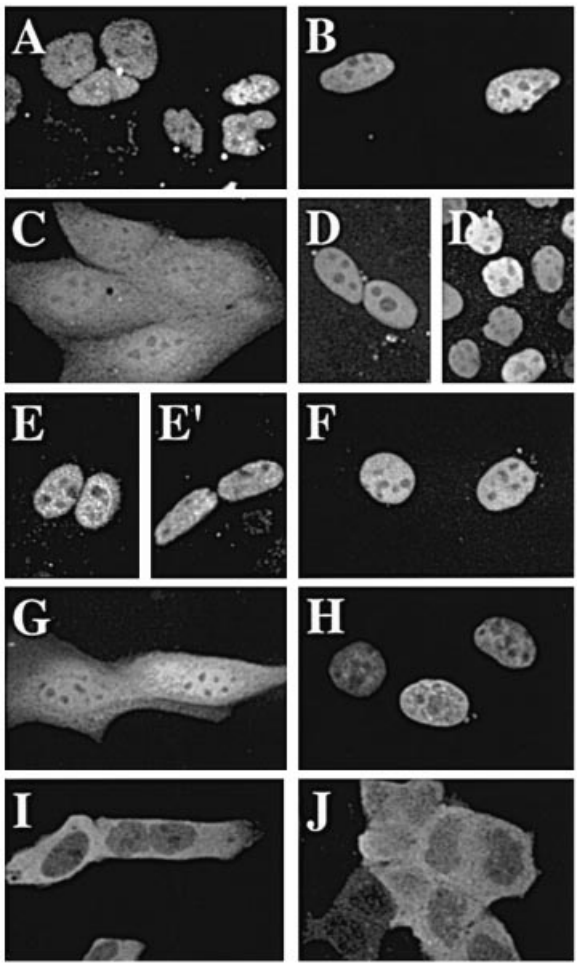

Figure 3 Nuclear localization of exogenously expressed kanadaptin fusion proteins

Localization of GFP- and His-tagged kanadaptin fusion proteins in transfected HEK-293 cells (**A**), HeLa cells (**B**) and MDCK cells (**C**–**J**). In all but (**E** and **E′**) cells were transiently transfected with kanadaptin-encoding plasmid constructs (see Figures 1B and 1C) and images were derived 24 h post-transfection in living cells. In the case of fusion proteins K1–ΔGFP (**E**) and K1–6 × His (**E′**), localization was determined by immunostaining in fixed cells using an antibody specific to kanadaptin and tetra-His respectively. MDCK cells shown in (**D′**) were stably transfected. Results for the expression plasmids are as follows: pGFP–K1 (**A**,**B**,**D** and **D′**), pEGFPC1 (expressing GFP alone) (**C**), pK1–ΔGFP (**E**), pK1–6 × His (**E′**), pGFP–K2 (**F**), pGFP–K3 (**G**), pGFP–K4 (**H**), pGFP–K5 (**I**) and pGFP–K6 (**J**; NLS1 mutant).

expression of kanadaptin, two expression vectors were derived from pK1–GFP. In the first case, the GFP cDNA was deleted to create expression vector pK1–ΔGFP (Figure 1B), in the second case the cDNA encoding GFP was replaced by an oligocassette encoding six histidine residues to create expression vector K1–6 × His (Figure 1C). After transient transfection, MDCK cells were fixed and the subcellular localization of K1–ΔGFP and K1–6 × His was visualized by immunofluorescence using anti-kanadaptin (Figure 3E) and anti-His (Figure 3E') antibodies respectively. Immunostaining in both cases was confined to the nucleus, thus confirming the results obtained with the GFP–K1 and K1–GFP fusion proteins. In the case of MDCK cells overexpressing K1–ΔGFP, kanadaptin-specific staining of nuclei was much brighter compared with that in non-transfected MDCK cells (results not shown).

As kanadaptin contains three potential NLS sequences (see Figure 1A), portions of kanadaptin were fused to GFP and transiently overexpressed in MDCK cells. In the first series of experiments, we investigated the subcellular localization of the C-terminally deleted GFP–kanadaptin fusion proteins GFP–K2 and GFP–K3 (Figure 1B). GFP–K3 differs from GFP–K2 in

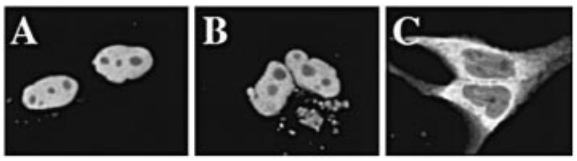

Figure 4 Kanadaptin NLS1 can target a heterologous protein to the nucleus

Localization of β-Gal–GFP fusion proteins in transiently transfected MDCK cells. Images showing GFP fluorescence in living cells were derived 24 h post transfection with β-Gal–NLS1–GFP (**A**), β-Gal–NP-NLS–GFP (**B**) or β-Gal–GFP (**C**).

that it lacks the N-terminal NLS (NLS1) (see Figure 1B), and in consequence was observed not to accumulate exclusively within the nucleus, but instead was evenly distributed throughout the cytoplasm and the nucleoplasm in comparable fashion with GFP alone (see Figure 3G), consistent with its small size (approx. 45 kDa), permitting free diffusion through the NPC. In contrast with GFP–K3, GFP–K2 showed strong nuclear accumulation (Figure 3F). To further investigate the role of NLS1 in targeting kanadaptin to the nucleus, GFP fusion proteins were constructed that either contain (GFP–K4) or lack (GFP–K5) the NLS1-containing region of kanadaptin that constitutes the difference between GFP–K2 and GFP–K3 (see Figure 1B). In these experiments, GFP–K4 (approx. 40 kDa) showed nuclear accumulation in MDCK cells (Figure 3H), whereas GFP–K5 (approx. 76 kDa) was excluded from the nucleus (Figure 3I). The nuclear accumulation of GFP–K4, which contains NLS1 but is small enough to diffuse freely through the NPC, implies that the approx. 10 kDa portion of kanadaptin may contain sequences capable of retaining kanadaptin within the nucleus by conferring binding to nuclear components (see below). The results indicate clearly that kanadaptin amino acids 140–230, which include NLS1, are necessary for nuclear localization of kanadaptin.

From the results for GFP–K5 and K5–GFP (results not shown), both of which contain both NLS2 and bpNLS but lack NLS1, we conclude that the NLS2 and bpNLS sequences play only a minor role in nuclear targeting of kanadaptin.

NLS1 is capable of targeting a heterologous protein to the nucleus

To examine whether NLS1 is sufficient to target a large heterologous protein into the nucleus, a plasmid was generated which expressed the fusion protein β-Gal–NLS1–GFP, containing kanadaptin amino acids 186–193 (^{186}AVSRKRKA) between the coding sequences of β-Gal and GFP. Fusion proteins either lacking (β-Gal–GFP) or containing a functional NLS (β-Gal–NP-NLS–GFP containing the bpNLS from nucleoplasmin served as controls. We found that subcellular localization of β-Gal–NLS1–GFP was similar to that of fusion protein β-Gal–NP-NLS–GFP in that NLS1, like NP-NLS, contained nuclear targeting activity (Figures 4A and 4B). As previously shown [10], β-Gal–GFP alone did not show any accumulation within the nucleus (Figure 4C). These results clearly demonstrate that NLS1 alone is sufficient to confer nuclear targeting to an otherwise cytoplasmically localized protein.

A single point mutation within NLS1 abolishes nuclear accumulation of kanadaptin

To confirm the direct involvement of NLS1 on nuclear import of kanadaptin, an expression vector (GFP–K6) was generated expressing an NLS mutant (Arg^{191} → Thr). Transient expression studies in MDCK cells, and other cell lines (HEK-293 and HeLa; results not shown) indicated that GFP–K6 was predominantly cytoplasmic (Figure 3J). Based on the effect of this single point mutation, we conclude that NLS1 is necessary for nuclear accumulation of kanadaptin.

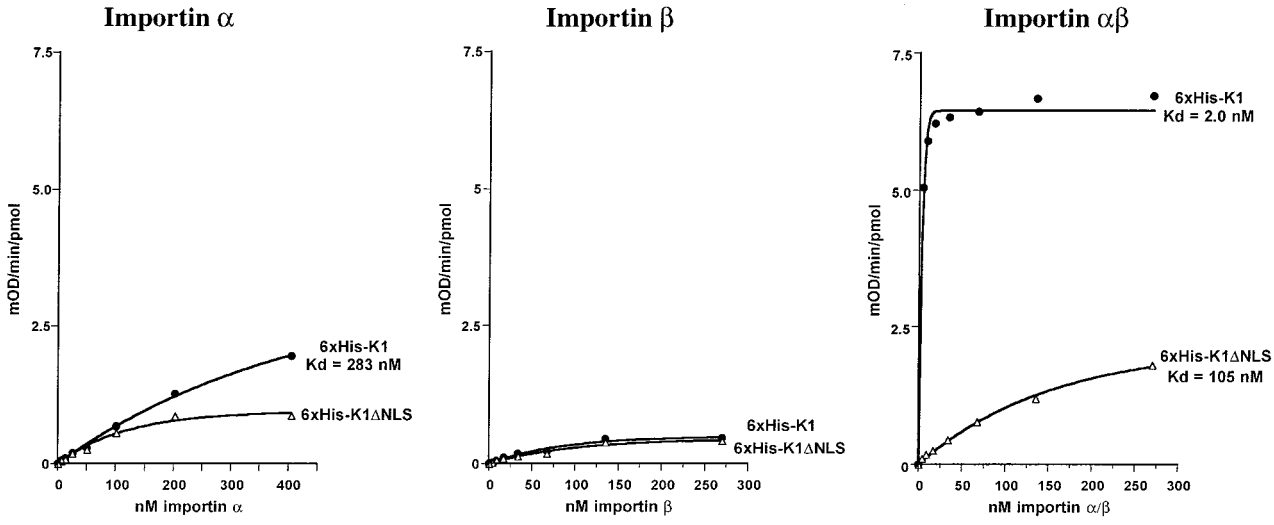

Figure 5 High affinity recognition of kanadaptin amino acids 1–231 by importin α/β

An ELISA-based binding assay was used in which fusion proteins 6 × His–K1 and 6 × His–K1ΔNLS1 were coated on to microtitre plates and incubated with increasing concentrations of the mouse importin subunits α, β or α/β, followed by successive incubation with primary and secondary antibodies, and chromogenic substrate. Curves for kinetic data were fitted to the function $B(x) = B_{max}(1 - e^{-kB})$, where x is the concentration of importin, k is the rate constant and B is the level of importin bound [16,18]. The results are from a single typical experiment performed in triplicate. The values for the apparent dissociation constant (K_d) representing the importin concentration yielding half-maximal binding are indicated. mOD, milli-absorbance.

Table 1 NLS binding parameters of bacterially expressed 6 × His–K1 and the NLS-mutated derivative (6 × His–K1ΔNLS1), measured using an ELISA-based binding assay

Importin binding parameters were determined from experimental data fitted as shown in Figure 5. Results for the apparent dissociation constant (K_d) and maximal level of binding (expressed relative to the binding to 6 × His-K1 by importin α/β) are expressed as means ± S.E.M. ($n = 3$ or 4). ND, K_d not able to be determined due to low importin binding.

	Importin binding parameters						
	Importin α		Importin β		Importin α/β		
Protein	K_d (nM)	B_{max} (% α/β)	K_d (nM)	B_{max} (% α/β)	K_d (nM)	B_{max} (% α/β)	n
6 × His–K1	203 ± 33	25.4 ± 3.1	ND	11.9 ± 1.4	4.5 ± 0.8	100	4
6 × His–K1ΔNLS1	440 ± 133	17.5 ± 1.4	ND	8.9 ± 2.2	116 ± 15	19.5 ± 3.1	3

NLS1 is recognized with high affinity by importin α/β

NLS1 resembles the T-ag NLS, which is recognized by the NLS receptor (i.e. the importin α/β heterodimer) through importin α. We postulated that nuclear targeting of kanadaptin might occur through the conventional importin α/β-dependent nuclear import pathway, and accordingly decided to employ an ELISA-based assay to test whether the fusion proteins 6 × His–K1 (carrying kanadaptin amino acids 1–231) and the 6 × His–K1ΔNLS1 derivative (containing the mutated NLS1) are recognized by the importin subunits. We found that 6 × His–K1 was recognized by importin α with fairly low affinity [Figure 5 and Table 1; apparent dissociation constant (K_d) of 203 nM], but not by importin β. The binding affinity of importin α to 6 × His–K1 was significantly increased in the presence of the importin β subunit (Figure 5 and Table 1; K_d of 4.5 nM), consistent with previous observations that the importin α–NLS interaction requires importin β to attain high affinity [16,18,24]. As expected, low affinity was observed for importin α/β binding to 6 × His–K1ΔNLS1 (Figure 5 and Table 1; K_d of 116 nM), demonstrating the specificity of binding for NLS1. These results indicate that kanadaptin NLS1 is recognized with high affinity by the importin α/β heterodimer, and that kanadaptin is therefore likely to follow a pathway of nuclear import similar to that of conventional NLS-containing proteins, such as T-ag [16,18], transcription factors, such as Dorsal [34] and signal transducer of transcription 1 ('STAT1') [42], and bpNLS-containing proteins, such as retinoblastoma protein [17] and *Xenopus laevis* phosphoprotein N1N2 [24].

Nuclear import kinetics of kanadaptin proteins *in vivo* and *in vitro*

Nuclear import kinetics of fluorescently labelled 6 × His–K1 and 6 × His–K1ΔNLS1 were measured in microinjected (Figure 6) and mechanically perforated HTC cells (Figure 7 and Table 2). Results were completely comparable in both systems in that 6 × His–K1 accumulated in the nucleus to levels more than 3–4 times those in the cytoplasm (Figures 6B and 7B, and Table 2). Half-maximal nuclear accumulation of microinjected 6 × His–K1 was achieved after approx. 1 and 2 min *in vivo* and *in vitro* respectively. The omission of cytosol from the *in vitro* assay reduced the rate of nuclear import more than 4-fold (half-life of approx. 8 min), indicating dependence on cytosolic factors. Consistent with the nM binding affinity of importin α/β to the NLS1 (Figure 5), specific antibodies to the importin subunits significantly reduced nuclear import of 6 × His–K1 both in terms of maximal accumulation (reduced by 20–40 %) and of the nuclear import rate (approx. 50 % slower, see Table 2). The cytosolic dependence of kanadaptin nuclear import could thus be

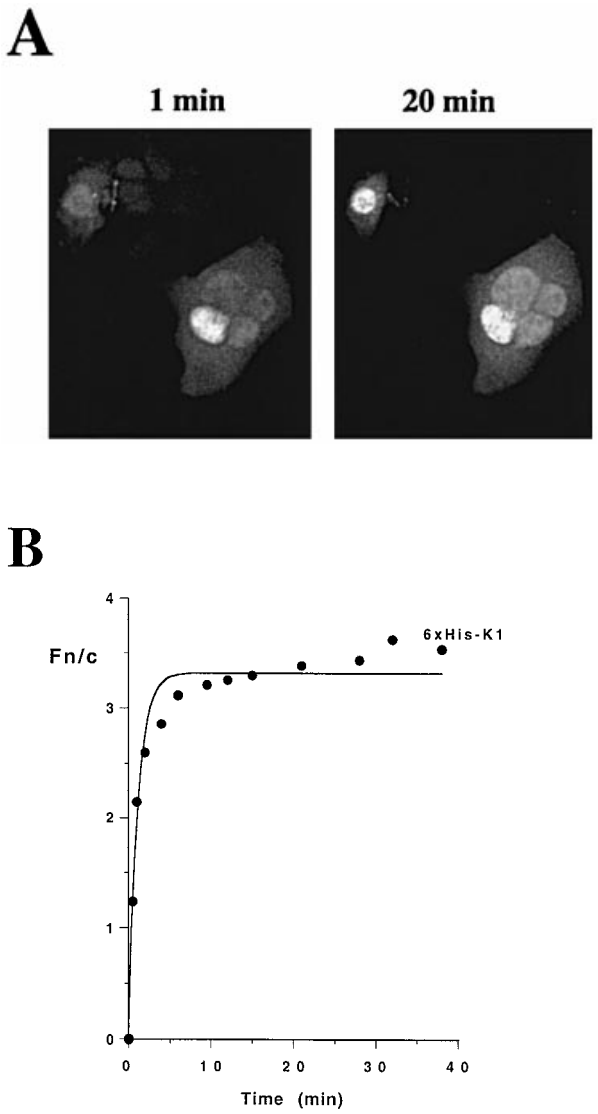

Figure 6 Nuclear import of kanadaptin fusion protein 6 × His–K1 *in vivo*

(**A**) Visualization of fluorescently labelled kanadaptin fusion protein 6 × His–K1 in microinjected HTC polykaryons at the time points indicated. (**B**) Nuclear import kinetics were determined as described in the Materials and methods section. Results are based on a single typical experiment where each point represents the average of 10–12 separate measurements for nuclear (Fn), cytoplasmic (Fc) and background (autofluorescence) fluorescence. Raw data were fitted to the function $Fn/c(t) = Fn/c_{max}(1 - e^{-kt})$, where t is time in minutes and k is the rate constant. Collated data are presented in Table 2.

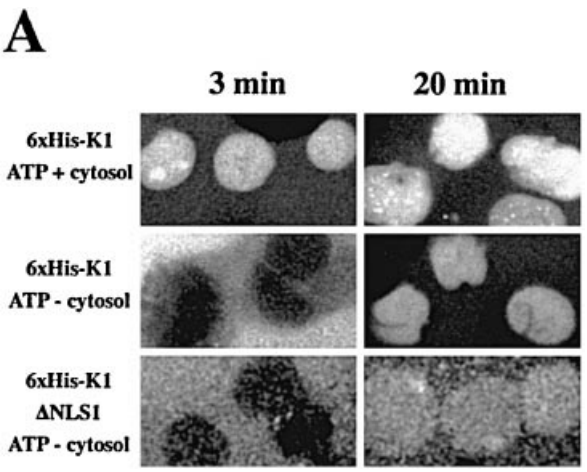

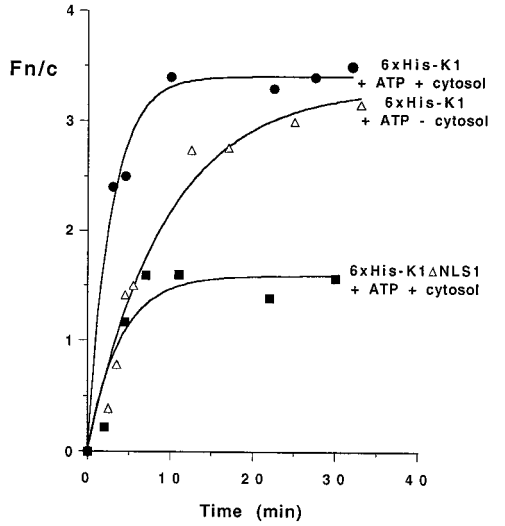

Figure 7 Nuclear import of kanadaptin fusion proteins *in vitro*

(**A**) Visualization of fluorescently labelled kanadaptin fusion protein 6 × His–K1 and NLS1 mutant variant in mechanically perforated HTC cells in the absence or presence of exogenously added cytosol and an ATP-regenerating system at the time points indicated. (**B**) Nuclear import kinetics were determined as described in the legend to Figure 6(B). Results are shown for a single typical experiment in which each point represents the average of up to 10 separate measurements for each of Fn, Fc and autofluorescence. Curve fitting was performed as described in the legend to Figure 6(B). Collated data are presented in Table 2.

Table 2 *In vitro* nuclear import kinetics of 6 × His–K1 compared with those of 6 × His–K1ΔNLS1

Raw data (see Figure 7B) were fitted to the function $Fn/c(t) = Fn/c_{max}(1 - e^{-kt})$, where t is time (min) and k is the rate constant. Results are presented as the means ± S.E.M. ($n = 3$, 4 or 9).

	Nuclear import parameter		
Protein	Fn/c_{max}	Half-life (min)	n
6 × His–K1			
+ ATP + cytosol	4.43 ± 0.31	1.95 ± 0.20	9
+ ATP − cytosol	3.77 ± 0.23	7.87 ± 2.40	4
+ ATP − cytosol + GTP[S]	3.67 ± 0.33	6.17 ± 0.73	3
+ ATP + cytosol + anti-(importin α)	3.23 ± 0.15	2.79 ± 1.10	3
+ ATP + cytosol + anti-(importin β)	2.85 ± 0.19	2.91 ± 0.33	4
6 × His–K1ΔNLS1			
+ ATP + cytosol	2.87 ± 0.38	4.27 ± 0.56	4

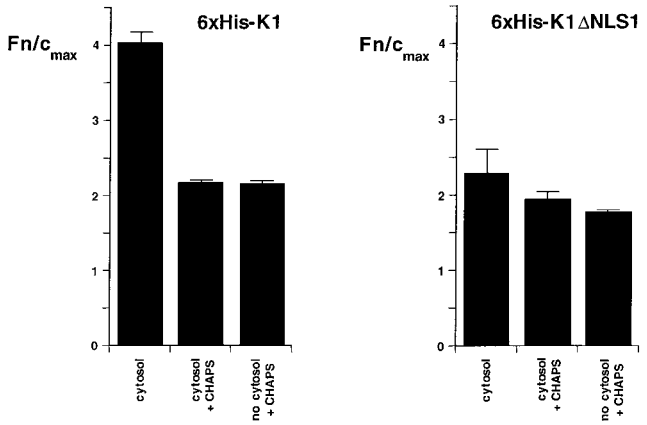

Figure 8 Nuclear accumulation of kanadaptin fusion proteins in the presence of the nuclear envelope-permeabilizing detergent CHAPS

Maximal nuclear accumulation of the kanadaptin fusion proteins 6 × His–K1 and 6 × His–K1ΔNLS1 was measured *in vitro* in the absence and presence of CHAPS and cytosol as indicated. The results represent averages from three separate experiments (± S.E.M.) performed as described in the legend to Figure 7(B).

attributed to the requirement for importin α/β; the involvement of the importin β-binding monomeric guanine nucleotide-binding protein Ran was implied by the observation that the non-hydrolysable GTP analogue GTP[S] reduced nuclear accumulation slightly, and slowed accumulation by more than 3-fold (Table 2).

That the nuclear accumulation was NLS1-dependent was indicated by the fact that 6 × His–K1ΔNLS1 showed significantly reduced maximal nuclear accumulation (approx. 40 %) compared with that of 6 × His–K1 (Figure 7 and Table 2). Since 6 × His–K1ΔNLS1 is below the cut-off for importin-dependent nuclear entry, its observed nuclear accumulation could be explained by its ability to be retained in the nucleus through binding to nuclear components [17,23]. To test for intranuclear binding, *in vitro* import measurements were carried out in the presence of the nuclear envelope-permeabilizing detergent CHAPS, which is known to perforate both the plasma membrane and the nuclear envelope, enabling molecules to diffuse freely into the nucleus; under these conditions, nuclear accumulation can only occur through binding to nuclear components. Both 6 × His–K1 and 6 × His–K1ΔNLS1 accumulated quite well in the nucleus in the presence of CHAPS, to levels that were approx. 2-fold those in the cytoplasm (Figure 8), with accumulation being independent of cytosol. The clear implication was that the nuclear accumulation of 6 × His–K1ΔNLS1 observed in the absence of CHAPS, and of 6 × His–K1 in the absence of cytosolic factors, could be attributed to the ability of the N-terminal region of kanadaptin to mediate binding in the nucleus. That 6 × His–K1ΔNLS1 showed nuclear accumulation comparable with that of 6 × His–K1 in the presence of CHAPS implied that NLS1 was not directly involved in mediating nuclear retention.

DISCUSSION

In the present study we report for the first time that the kAE1-binding protein, kanadaptin, is a multidomain protein capable of accumulating in the nucleus of various epithelial and non-epithelial cultured cell types. Our findings contrast with the results of Chen et al. [1], who reported vesicular cytoplasmic immunolocalization of kanadaptin in type A intercalated cells of rabbit kidney collecting ducts. With respect to the possible role of kanadaptin in type A intercalated cells, it was proposed that kanadaptin might be involved in targeting of kAE1-containing post-Golgi carrier vesicles to the basolateral plasma membrane. However, our recent analyses in rat kidney tissue sections indicate kanadaptin-specific nuclear and cytoplasmic granular-like staining in a large variety of different cell types, most intensely in epithelial cells of the proximal tubule. We did not see any significant immunostaining of intercalated cells of the collecting ducts in rats. These obvious differences must be attributed either to the fact that the observations of Chen et al. [1] in the rabbit cannot be extrapolated to other species, or that our antibody does not recognize vesicle-bound kanadaptin in intercalated cells. Another interpretation of these discrepencies would be that the lack of cytoplasmic immunostaining in intercalated cells of the rat is due to the fact that in rats cytoplasmic kAE1-containing vesicles are rather rare compared with cortical intercalated cells in the rabbit [43,44]. Therefore it is difficult at the present stage to discuss the specific role of kanadaptin in intercalated cells. However, the wide expression of kanadaptin in many cells and tissues not expressing kAE1 clearly suggests additional and more general functions for kanadaptin not related to kAE1. Our subcellular localization studies using an array of different GFP–kanadaptin fusion proteins demonstrate NLS1 (AVSRKRKA^{193}) to be sufficient and necessary for the nuclear translocation of kanadaptin. Other NLS-like motifs within kanadaptin's sequence (bpNLS and NLS2) seem to have only a minor role in nuclear translocation of kanadaptin. Employing an ELISA-based binding assay, we demonstrate that the NLS1-containing 231-amino-acid long N-terminal portion of kanadaptin is recognized with high affinity by the importin α/β heterodimer. This is consistent with our observation that nuclear accumulation of $6\times$His–K1 *in vitro* depended on cytosolic components and could be inhibited by importin antibodies. That nuclear accumulation of kanadaptin depends on a functional NLS1 is indicated by the fact that a single point mutation of NLS1 (Arg^{191} → Thr) abolished nuclear import of kanadaptin in transfected cells. Moreover, this mutation reduced both nuclear import *in vitro* and recognition by importin α/β. In addition to NLS1, a nuclear retention sequence appears to be present within amino acids 140–230, as indicated by nuclear accumulation of the 40 kDa fusion protein GFP–K4 (Figure 3H) and the ability of $6\times$His–K1ΔNLS1 to accumulate in the nucleus in the absence of an intact nuclear envelope (Figure 8). This nuclear retention also explains the observation that nuclear accumulation of $6\times$His–K1 *in vitro* is not completely abolished by importin antibodies, the absence of cytosol, or the presence of the non-hydrolysable GTP analogue GTP[S].

In conclusion, kanadaptin appears to be a karyophilic protein, able to reside within both the nucleus, through NLS- and importin-dependent nuclear import and nuclear retention, and in the cytoplasm ([1], and results not shown). However, the role of kanadaptin in the nucleus and in non-kAE1-expressing cells remains to be elucidated.

We are indebted to Mrs Martina Koch, Mr Holger Gößmann and Mrs Chenoa Barton for skilled technical assistance, to Dr Thomas Stamminger for providing the β-Gal–GFP expression plasmids, and to Professor Qais Al-Awqati for making the kanadaptin cDNA available. We also thank Dr Birgit Drabent for providing the mouse histone H1.2 antibody and to Dr Uwe Borgmeyer for providing the NT2/D1 cells. This work was supported by grants of the Deutsche Forschungsgemeinschaft (Hu 621/3-1 to S.H.; SFB 176).

REFERENCES

1 Chen, J., Vijayakumar, S., Li, X. and Al-Awqati, Q. (1998) Kanadaptin is a protein that interacts with the kidney but not the erythroid form of band 3. J. Biol. Chem. **273**, 1038–1043
2 Drenckhahn, D., Schlüter, K., Allen, D. P. and Bennett, V. (1985) Colocalization of band 3 with ankyrin and spectrin at the basal membrane of intercalated cells in the rat kidney. Science (Washington, D.C.) **230**, 1287–1289
3 Kudrycki, K. E. and Shull, G. E. (1989) Primary structure of the rat kidney band 3 anion exchange protein deduced from a cDNA. J. Biol. Chem. **264**, 8185–8192
4 Kudrycki, K. E. and Shull, G. E. (1993) Rat kidney band 3 Cl^-/HCO_3^- exchanger mRNA is transcribed from an alternative promoter. Am. J. Physiol. **264**, F540–F547
5 Brosius, III, F. C., Alper, S. L., Garcia, A. M. and Lodish, H. F. (1989) The major kidney band 3 gene transcript predicts an amino-terminal truncated band 3 polypeptide. J. Biol. Chem. **264**, 7784–7787
6 Kollert-Jöns, A., Wagner, S., Hübner, S., Appelhans, H. and Drenckhahn, D. (1993) Anion exchanger 1 in human kidney and oncocytoma differs from erythroid AE1 in its NH_2 terminus. Am. J. Physiol. **265**, F813–F821
7 Brown, D., Hirsch, S. and Gluck, S. (1988) Localization of a proton-pumping ATPase in rat kidney. J. Clin. Invest. **82**, 2114–2126
8 Görlich, D. (1997) Nuclear protein import. Curr. Opin. Cell Biol. **9**, 412–419
9 Imamoto, N., Kamei, Y. and Yoneda, Y. (1998) Nuclear transport factors: function, behavior and interaction. Eur. J. Histochem. **42**, 9–20
10 Sorg, G. and Stamminger, T. (1999) Mapping of nuclear localization signals by simultaneous fusion to green fluorescent protein and to β-galactosidase. BioTechniques **26**, 858–862
11 Chen, C. and Okayama, H. (1987) High-efficiency transformation of mammalian cells by plasmid DNA. Mol. Cell. Biol. **7**, 2745–2752
12 Jans, D. A., Ackermann, M. J., Bischoff, J. R., Beach, D. H. and Peters, R. (1991) p34cdc2-mediated phosphorylation at T124 inhibits nuclear import of SV-40 T antigen proteins. J. Cell Biol. **115**, 1203–1212
13 Rihs, H. P., Jans, D. A., Fan, H. and Peters, R. (1991) The rate of nuclear cytoplasmic protein transport is determined by the casein kinase II site flanking the nuclear localization sequence of the SV40 T-antigen. EMBO J. **10**, 633–639
14 Bradford, M. M. (1976) A rapid and sensitive method for the quantitation of microgram quantities of protein utilizing the principle of protein-dye binding. Anal. Biochem. **72**, 248–254
15 Imamoto, N., Shimamoto, T., Takao, T., Tachibana, T., Kose, S., Matsubae, M., Sekimoto, T., Shimonishi, Y. and Yoneda, Y. (1995) *In vivo* evidence for involvement of a 58 kDa component of nuclear pore-targeting complex in nuclear protein import. EMBO J. **14**, 3617–3626
16 Hübner, S., Xiao, C. Y. and Jans, D. A. (1997) The protein kinase CK2 site ($Ser^{111/112}$) enhances recognition of the simian virus 40 large T-antigen nuclear localization sequence by importin. J. Biol. Chem. **272**, 17191–17195
17 Efthymiadis, A., Shao, H., Hübner, S. and Jans, D. A. (1997) Kinetic characterization of the human retinoblastoma protein bipartite nuclear localization sequence (NLS) *in vivo* and *in vitro*. A comparison with the SV40 large T-antigen NLS. J. Biol. Chem. **272**, 22134–22139
18 Xiao, C. Y., Hübner, S. and Jans, D. A. (1997) SV40 large tumor antigen nuclear import is regulated by the double-stranded DNA-dependent protein kinase site (serine 120) flanking the nuclear localization sequence. J. Biol. Chem. **272**, 22191–22198
19 Jans, D. A. (1992) The mobile receptor hypothesis revisited: a mechanistic role for hormone receptor lateral mobility in signal transduction. Biochim. Biophys. Acta **1113**, 271–276
20 Jans, D. A. (1995) The regulation of protein transport to the nucleus by phosphorylation. Biochem. J. **311**, 705–716
21 Jans, D. A., Peters, R., Zsigo, J. and Fahrenholz, F. (1989) The adenylate cyclase-coupled vasopressin V2-receptor is highly laterally mobile in membranes of LLC-PK1 renal epithelial cells at physiological temperature. EMBO J. **8**, 2481–2488
22 Jans, D. A., Peters, R. and Fahrenholz, F. (1990) Lateral mobility of the phospholipase C-activating vasopressin V1-type receptor in A7r5 smooth muscle cells: a comparison with the adenylate cyclase-coupled V2-receptor. EMBO J. **9**, 2693–2699
23 Efthymiadis, A., Briggs, L. J. and Jans, D. A. (1998) The HIV-1 Tat nuclear localization sequence confers novel nuclear import properties. J. Biol. Chem. **273**, 1623–1628
24 Hübner, S., Smith, H. M., Hu, W., Chan, C. K., Rihs, H. P., Paschal, B. M., Raikhel, N. V. and Jans, D. A. (1999) Plant importin α binds nuclear localization sequences with high affinity and can mediate nuclear import independent of importin β. J. Biol. Chem. **274**, 22610–22617

25 Bairoch, A. (1993) The PROSITE dictionary of sites and patterns in proteins, its current status. Nucleic Acids Res. **21**, 3097–3103
26 Bairoch, A., Bucher, P. and Hofmann, K. (1997) The PROSITE database, its status in 1997. Nucleic Acids Res. **25**, 217–221
27 Schultz, J., Milpetz, F., Bork, P. and Ponting, C. P. (1998) SMART, a simple modular architecture research tool: identification of signaling domains. Proc. Natl. Acad. Sci. U.S.A. **95**, 5857–5864
28 Schultz, J., Copley, R. R., Doerks, T., Ponting, C. P. and Bork, P. (2000) SMART: a web-based tool for the study of genetically mobile domains. Nucleic Acids Res. **28**, 231–234
29 Cohen, G. B., Ren, R. and Baltimore, D. (1995) Modular binding domains in signal transduction proteins. Cell (Cambridge, Mass.) **80**, 237–248
30 Kalderon, D., Roberts, B. L., Richardson, W. D. and Smith, A. E. (1984) A short amino acid sequence able to specify nuclear location. Cell (Cambridge, Mass.) **39**, 499–509
31 Kalderon, D., Richardson, W. D., Markham, A. F. and Smith, A. E. (1984) Sequence requirements for nuclear location of simian virus 40 large-T antigen. Nature (London) **311**, 33–38
32 Lanford, R. E. and Butel, J. S. (1984) Construction and characterization of an SV40 mutant defective in nuclear transport of T antigen. Cell (Cambridge, Mass.) **37**, 801–813
33 Robbins, J., Dilworth, S. M., Laskey, R. A. and Dingwall, C. (1991) Two interdependent basic domains in nucleoplasmin nuclear targeting sequence: identification of a class of bipartite nuclear targeting sequence. Cell (Cambridge, Mass.) **64**, 615–623
34 Briggs, L. J., Stein, D., Goltz, J., Corrigan, V. C., Efthymiadis, A., Hübner, S. and Jans, D. A. (1998) The cAMP-dependent protein kinase site (Ser^{312}) enhances dorsal nuclear import through facilitating nuclear localization sequence/importin interaction. J. Biol. Chem. **273**, 22745–22752
35 Hicks, G. R., Smith, H. M., Lobreaux, S. and Raikhel, N. V. (1996) Nuclear import in permeabilized protoplasts from higher plants has unique features. Plant Cell **8**, 1337–1352
36 Hu, W. and Jans, D. A. (1999) Efficiency of importin α/β-mediated nuclear localization sequence recognition and nuclear import. Differential role of NTF2. J. Biol. Chem. **274**, 15820–15827
37 Smith, H. M., Hicks, G. R. and Raikhel, N. V. (1997) Importin α from *Arabidopsis thaliana* is a nuclear import receptor that recognizes three classes of import signals. Plant Physiol. **114**, 411–417
38 Jans, D. A. and Hübner, S. (1996) Regulation of protein transport to the nucleus: central role of phosphorylation. Physiol. Rev. **76**, 651–685
39 Hübner, S., Jans, D. A. and Drenckhahn, D. (2001) Roles of cytoskeletal and junctional plaque proteins in nuclear signalling. Int. Rev. Cytol. **208**, 207–249
40 Saier, Jr, M. H. (1981) Growth and differentiated properties of a kidney epithelial cell line (MDCK). Am. J. Physiol. **240**, C106–C109
41 Valentich, J. D. (1981) Morphological similarities between the dog kidney cell line MDCK and the mammalian cortical collecting tubule. Ann. N. Y. Acad. Sci. **372**, 384–405
42 Sekimoto, T., Imamoto, N., Nakajima, K., Hirano, T. and Yoneda, Y. (1997) Extracellular signal-dependent nuclear import of Stat1 is mediated by nuclear pore-targeting complex formation with NPI-1, but not Rch1. EMBO J. **16**, 7067–7077
43 Verlander, J. W., Madsen, K. M., Low, P. S., Allen, D. P. and Tisher, C. C. (1988) Immunocytochemical localization of band 3 protein in the rat collecting duct. Am. J. Physiol. **255**, F115–F125
44 Madsen, K. M., Kim, J. and Tisher, C. C. (1992) Intracellular band 3 immunostaining in type A intercalated cells of rabbit kidney. Am. J. Physiol. **262**, F1015–F1022
45 Nakai, K. and Kanehisa, M. (1992) A knowledge base for predicting protein localization sites in eukaryotic cells. Genomics **14**, 897–911

Received 9 July 2001/5 October 2001; accepted 1 November 2001